LONG TERM AGING EFFECTS ON THE RELIABILITY OF LEAD FREE SOLDER JOINTS IN BALL GRID ARRAY PACKAGES WITH VARIOUS PITCH SIZES AND BALL ALIGNMENTS

Cong Zhao, Chaobo Shen, Zhou Hai, Jiawei Zhang, M. J. Bozack, and J. L. Evans
Center for Advanced Vehicle and Extreme Environment Electronics (CAVE^3)
Auburn University
Auburn, AL, USA
czz0025@auburn.edu

ABSTRACT
This paper investigates the impact of isothermal aging on the long-term reliability of lead-free solder joints. The full experimental matrix contains SAC105 and SAC305 solder alloys assembled in ball grid arrays (BGAs) with package sizes ranging from 19mm, 0.8mm pitch to 5mm, 0.4mm pitch, and three surface platings (ImAg, ENIG, and ENEPIG). The test specimens were subjected to isothermal aging at temperatures 25°C, 55°C, 85°C to 125°C with aging times of 0, 6 months, 12 months and 24 months, followed by accelerated thermal cycling from -40°C to 125°C. A two-parameter Weibull plot shows the reliability degrades up to 70% after two years of aging at elevated temperature. The degradation *rate* slows with aging time. The degradation is greater with smaller solder joints and perimeter ball alignments when compared to large-diameter solder balls and full array ball alignments. The thickness of the Cu-Sn intermetallic layer (IMC) layer during the testing grows with an approximate ~ $t^{0.5}$ dependence (diffusion-controlled reaction) during isothermal aging + thermal cycling.

Key words: SAC105, SAC305, reliability, aging, pitch size, solder ball alignment

INTRODUCTION
Almost a decade ago, WEEE (Waste Electrical and Electronic Equipment) and RoHS (Restriction of Hazardous Substances) legislation was implemented in Europe to avoid using eutectic Sn-37Pb solder in electronics. This resulted in tremendous interest in electronics manufacturing based on Pb-free materials. Among many Pb-free alloys, Sn-Ag-Cu (SAC) has become the leading candidate. Considerable work has been done to investigate the thermal properties of Pb-free systems, with the results showing that exposure to temperature excursions causes thermal fatigue of SAC solder joints, leading to failure of the electronics. Solder deformation occurs during thermal aging and cycling, caused by coefficient of thermal expansion (CTE) mismatches between the solder joint, the printed circuit board (PCB), and the component, as well as local CTE differences between grains within the solder [1]. The joint reliability is also influenced by intermetallic (IMC) layer growth at the PCB/solder joint/package interface, growth of second phase compounds in the bulk of the alloy and/or along the grain boundaries in the solder [2][3]. The solder additionally experiences plastic work and recrystallization during thermal cycling, which encourages crack propagation in the solder bulk. An example is given by Lee, et al. [4] who investigated the interaction between isothermal aging and the reliability of fine-pitch BGAs of Sn-3.0Ag-0.5Cu (SAC305) solder interconnects. They found that the package lifetime reduced by 44% during aging at 150°C, but aging at 100°C had less effect on package lifetime.

Hundreds of technical papers have dealt with the thermal-mechanical properties of Pb-free systems; however, few works have addressed the package characteristic lifetime reliability during long-term isothermal aging at elevated temperatures, which is the focus of this study. Previously Zhang, et al. [5-7] observed a dramatic negative effect on fine-pitch ball grid array (BGA) packaging reliability during isothermal aging with Sn-1.0Ag-0.5Cu (SAC105) and Sn-3.0Ag-0.5Cu (SAC305) solder ball interconnects. Significant package lifetime degradation in accelerated thermal cycling tests was observed for both SAC105 and SAC305 in 19mm, and 5mm BGA packages, with aging at 25°C, 55°C, 85°C, and 125°C and 6 months and 12 months of aging time. Failure analysis showed significant bulk Ag_3Sn coarsening and intermetallic Cu_6Sn_5 growth at the solder joint interfaces. Then Hai, et al. [8] investigated the reliability of SAC105 and SAC305 solder joints in 10mm BGA packages (ImAg plating) under isothermal aging at 125°C up to 24 months, followed by Shen, et al. [9] who focused on the reliability of 15mm BGA on ENIG/ENEPIG platings during aging at 125°C for up to 12 months. Both studies concluded that SAC305 performs better than SAC105 under most platings and aging condition combinations. Failure analysis showed continuous growth of Cu-Sn IMC in SAC/ImAg solder-plating system, as well as Cu-Ni-Sn IMC in SAC/ENIG/ENEPIG systems during thermal aging, with cycling finally causing solder joint fatigue failure.

In this paper, we extend our prior work on SAC alloys [5,6] by including a wider array of package sizes, pitch sizes, and surface platings, using isothermal aging times up to 24 months and a range of isothermal aging temperatures up to 125°C.

EXPERIMENT

The assembled test vehicle was based on a four-layer FR-406 glass epoxy PCB with a glass transition temperature of 170°C. The dimensions of the board were 100.076 x 67.056 mm with a thickness of 1.574 mm (measured laminate to laminate). The BGA components were mounted on the PCB by SAC105 and SAC305 solder joints with package sizes 5x5mm, 10x10mm, 15mmx15mm, and 19mmx19mm as well as two pitch sizes 0.8mm and 0.4mm. Non-solder mask design (NSMD) pads were used. The copper pads were plated by three surface finishes: ImAg, ENIG, and ENEPIG. The test component matrix is shown in Table 1. Figure 1 shows a schematic of the test vehicle.

Table 1. Test Component Matrix

Package Size (mm)	Ball Count	Ball Diameter (mm)	Pitch Size (mm)	Ball Alignment
19x19	288	0.38	0.8	Perimeter
15x15	208	0.36	0.8	Perimeter
10x10	360	0.18	0.4	Perimeter
5x5	97	0.20	0.4	Full Array

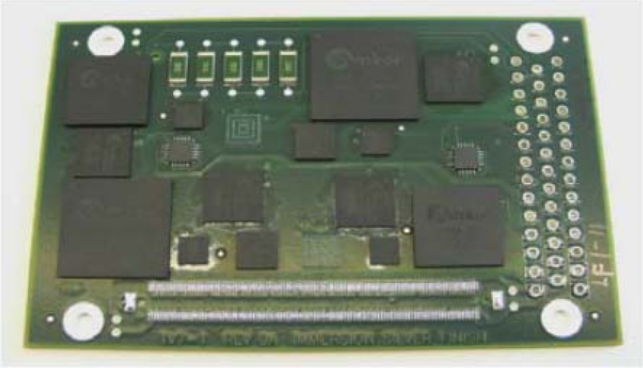

Figure 1. Assembled Test Vehicle

All test components were wired in daisy chain, which allowed for continuous sampling of component reliability during accelerated life tests. The test vehicles were grouped by aging temperature, from 25°C, 55°C, 85°C to 125°C with aging times of 0, 6 months, 12 months and 24 months. Subsequently, all test PCBs were placed vertically in an accelerated thermal cycling chamber and wired out to a data acquisition system developed by CAVE3. The system consists of a switch scanning system coupled with a high accuracy digital multi-meter, which allows for real-time measurement of the resistance change of the daisy chain. Based on the IPC-9701 standard, the practical definition of solder joint failure is the interruption of electrical continuity > 1000 ohms. In this study, we defined "failure" to occur when the daisy chain resistance was > 300 ohms for 5 sequential resistance measurements. Table 2 shows the number of PCBs allotted in the thermal aging test plan.

Table 2. Thermal Aging Test Plan

Aging Time / Aging Temp.	No Aging			6 months			12 months			24 months
	ImAg	ENIG	ENEPIG	ImAg	ENIG	ENEPIG	ImAg	ENIG	ENEPIG	ImAg
25℃	8	5	5	5			5			5
55℃				5			5			5
85℃				5			5			5
125℃				5	15	15	5	10	10	5

The thermal cycle test was from -40°C to 125°C with 15 minutes dwell time and 30 minutes ramp time. Figure 2 shows the thermal cycling profile.

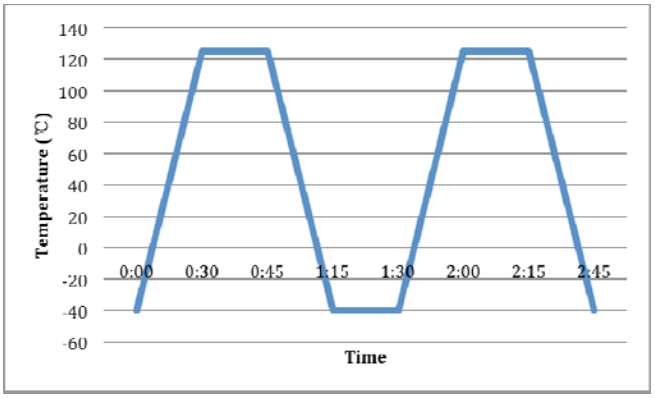

Figure 2. Thermal Cycling Profile

The failure data are reported using a two-parameter Weibull analysis. All samples for microscopic examination were cross sectioned and grinded with SiC polishing paper (240, 320, 400, 600, 800, 1200) followed by two-steps of fine polishing with 3 micron diamond suspension. Failure analysis proceeded by recording back-scattered electron (BSE) images of representative failed solder cross-sections after the tests.

RESULTS AND DISCUSSION

Data Analysis

A two-parameter (η, β) Weibull distribution was used to characterize the failure life of the electronic packages. The characteristic life η is the point (i.e., the number of cycles) at which 63.21% of the population is expected to fail, and the slope β distinguishes different failure modes. The least squares method was used to estimate η and β of the Weibull distribution and the r^2 value indicates the quality of the data fit.

In our previous study [8,9] the reliability for 10mm and 15mm BGA packages with SAC105/305 solder alloys and different surface finishes aged at 125°C for up to 12 months showed significant characteristic life degradation. Similar trends are observed here for SAC 105, 305 19mm BGA packages at 12 months and for longer aging times over a variety of aging temperatures. For example, Figure 3 shows Weibull plots for the ImAg, 19mm BGA with aging temperatures from 25°C, 55°C, 85°C to 125°C up to 24 months. Figure 3a, 3b are for 6 months aging; Figure 3c, 3d are for 12 months aging, and Figure 3e, 3f are for aging at 125°C up to 24 months.

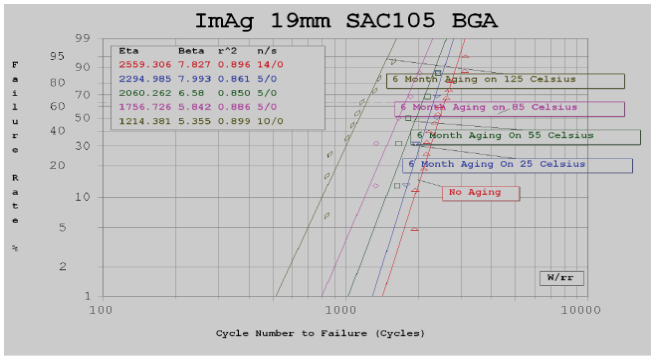

(a)

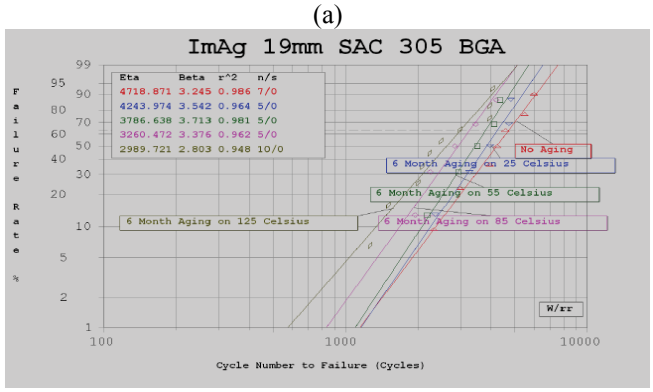

(b)

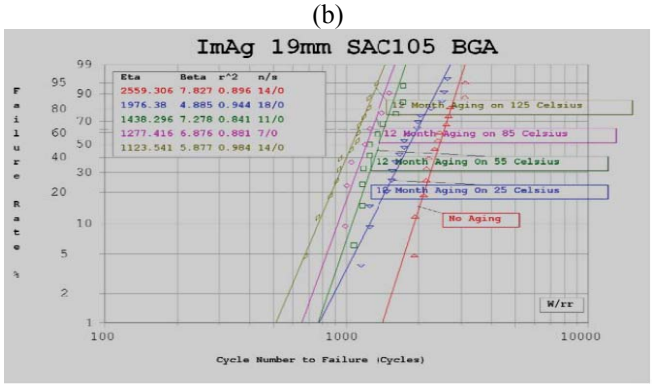

(c)

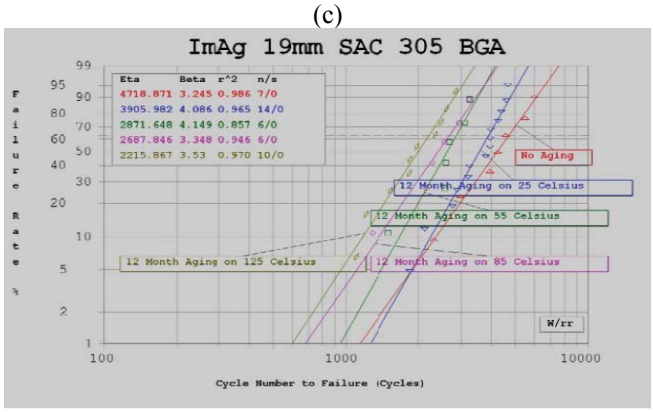

(d)

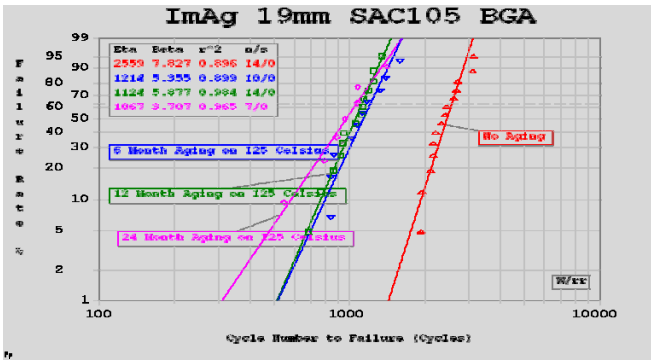

(e)

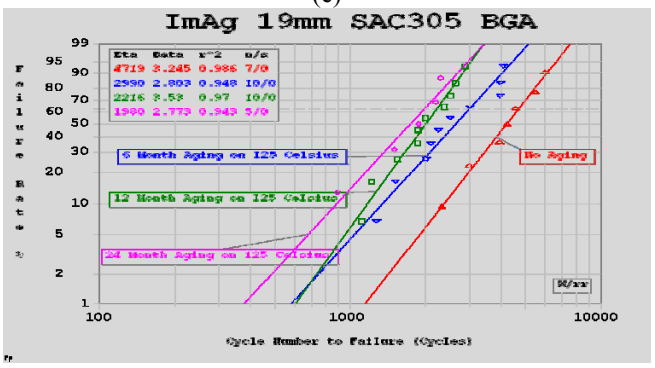

(f)

Figure 3. Weibull plots for the ImAg 19mm BGA: (a) SAC105 6 months aging; (b) SAC305 6 months aging; (c) SAC105 12 months aging; (d) SAC305 12 months aging; (e) SAC105 aging at 125°C up to 24 months; (f) SAC305 aging at 125°C up to 24 months

To illustrate the Weibull data more clearly, we construct a characteristic life degradation chart (η vs. aging time) based on the Weibull plots. Figure 4 shows a degradation chart for the ImAg 19mm BGA aged at 125°C.

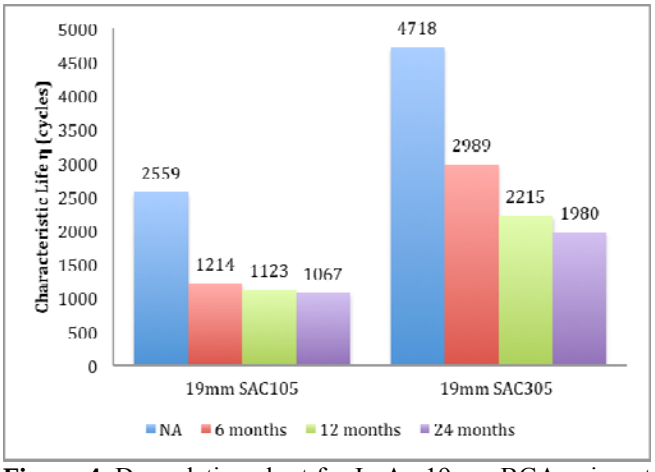

Figure 4. Degradation chart for ImAg 19mm BGA aging at 125°C with varying aging times (NA = No Aging)

From Figure 4 it is readily observed that for the 19mm SAC105 BGA after 24 months aging, the characteristic lifetime is reduced to 1067 cycles, which is a 58.3% degradation compared to 2559 cycles for no aging group. For 12 months and 6 months aging, the degradation rates are

56.1% and 52.5%, respectively. Similarly, for SAC305 the characteristic lifetime degrades 58% after 24 months aging, 53% after 12 months aging, and 36.6% after 6 months aging.

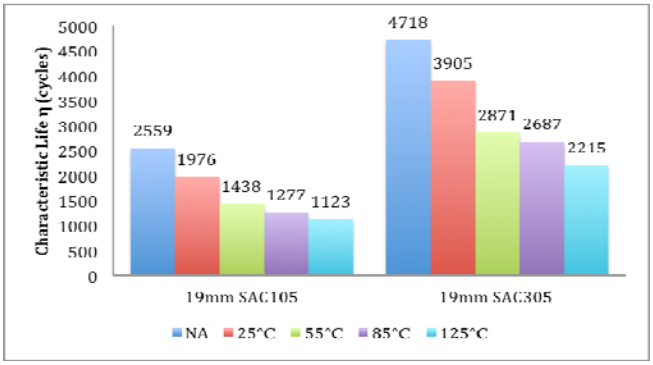

Figure 5. Degradation chart for ImAg 19mm BGA reliability, after 12 months of aging at varying aging temperatures.

By fixing the aging time and varying the aging temperature, the reliability trend vs. aging temperature for the ImAg 19 mm BGA is seen in Figure 5. For the 19mm SAC105 BGA subjected to 12 months aging at 125°C, the characteristic lifetime was reduced to 1123 cycles, which is a 56.1% degradation, compared to 2559 cycles for no aging group. For 85°C, 55°C, and 25°C, the degradation rates are 50.1%, 43.8% and 22.7%, respectively. Similarly, for SAC305, the characteristic lifetime degrades 53% at 125°C aging temperature, 43% at 85°C, 39.1% at 55°C, and 17.2% at 25°C. For other BGA components in the test matrix, having different package sizes and surface platings the trends of reliability degradation are similar. Clearly, the reliability of BGA components subjected to isothermal aging suffer dramatic degradation with longer aging times and higher aging temperatures.

Table 3 illustrates how the degradation *rate* slows with aging time. The solders experience a high rate of degradation over the first six months of aging, which slows dramatically with additional aging time.

Table 3. Characteristic Life for BGA for Different Aging Times (aging at 125°C; M = months)

Aging Time	19mm SAC105	19mm SAC305	15mm SAC105	15mm SAC305	10mm SAC105	10mm SAC305	5mm SAC105	5mm SAC305
No Aging	2559	4718	2925	3742	2418	3328	4841	5170
6 M	1214	2989	1429	2082	1115	2082	2383	3209
12 M	1123	2215	1324	1884	1079	1551	2268	3012
24 M	1067	1980	1106	1516	944	1338	2021	2617

For example, for the 19mm SAC105 BGA after 6 months of aging, the characteristic life lowers to 1214 cycles, which is a 52.6% degradation compared to 2559 cycles for the no-aging group. Then, after 12 months of aging, the characteristic life is reduced to 1123 cycles, which is a 56.1% degradation compared to no aging group. Hence, 6 months of additional aging yields only 3.5% more degradation or failure. The degradation rate for all tested alloys/pitch sizes is shown in Table 4. Differences between the degradation rate with aging time is shown is Table 5.

Table 4. Degradation Rate of Each Aging Group (M = months)

Aging Period	19mm SAC105	19mm SAC305	15mm SAC105	15mm SAC305	10mm SAC105	10mm SAC305	5mm SAC105	5mm SAC305
0 to 6 M	52.6%	36.6%	51.1%	44.4%	53.9%	37.4%	50.8%	37.9%
0 to 12M	56.1%	53.1%	54.7%	49.7%	55.4%	53.4%	53.2%	41.7%
0 to 24 M	58.3%	58.0%	62.2%	59.5%	61.0%	59.8%	58.3%	49.4%

Table 5. Degradation Rate Differences with Aging Time (M = months)

Aging Period	19mm SAC105	19mm SAC305	15mm SAC105	15mm SAC305	10mm SAC105	10mm SAC305	5mm SAC105	5mm SAC305
0 to 6 M	52.6%	36.6%	51.1%	44.4%	53.9%	37.4%	50.8%	37.9%
6 to 12M	3.6%	16.4%	3.6%	5.3%	1.5%	16.0%	2.4%	3.8%
12 to 24 M	2.2%	5.0%	7.5%	9.8%	5.6%	6.4%	5.1%	7.6%

From Table 5 we conclude that for each of the aging groups, during the first time period of 6 months the components reliability degrades in a very fast rate (over 50%). With additional aging time after 6 months, however, the degradation rate becomes slower and slower (< 10%) and eventually may approach an asymptotic value. Clearly, the degradation rate obeys a rapid reduction for early aging times, followed by a transition to linear behavior.

The relationship between failure and package pitch size and ball alignment is shown in Table 6, which illustrates the characteristic life for SAC 305 BGA (aging at 125°C) with varying package sizes.

Table 6. Characteristic Life for SAC 305 BGA Aging at 125°C with Varying Package Sizes (M = months; NA = not aged)

Package Size \ Aging Time	NA	6M	12M	24M
19	4718	2989	2215	1980
15	3742	2082	1884	1516
10	3328	1739	1551	1338
5	5170	3209	3012	2617

A complementary viewpoint of the data is given in Figure 6.

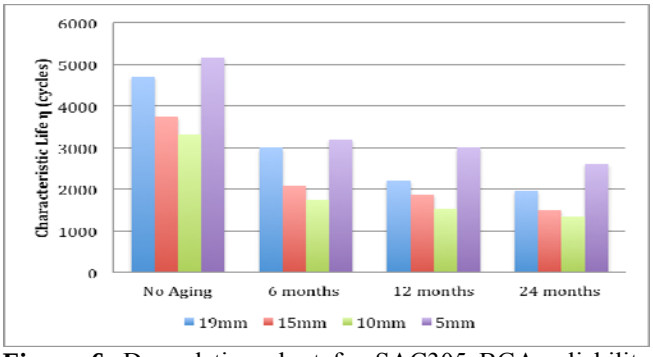

Figure 6. Degradation chart for SAC305 BGA reliability after aging at 125°C using varying package sizes.

From Table 1, the 19mm and 15mm BGAs have a pitch size of 0.8mm, while the 10mm and 5mm BGAs have a 0.4mm pitch size. The ball diameter for 19mm BGA is 0.38mm; for 15mm it is 0.36mm; for 10mm it is 0.18mm; and for 5mm it is 0.20mm. The 19mm, 15mm, and 10mm BGAs have a perimeter ball alignment, while 5mm BGA have full array ball alignment. Figure 6 discloses that, for perimeter ball alignments, the 19mm and 15mm BGAs always have higher characteristic lifetimes than the 10mm, which shows that packages with large solder balls have higher reliability. On the other hand, the 5mm BGA has the highest characteristic life, indicating that packages with full array ball alignments perform better than perimeter ball alignments under high temperature aging + thermal cycling conditions. This implies that the full array ball alignment has higher structural stability from the mechanical point of view, so that solder balls can endure severe changes of stress and strain during thermal fatigue caused by CTE mismatches. It thus appears to be possible to improve the overall electronic reliability by adding some 'dummy solder balls' to change from a perimeter ball alignment to a full array ball alignment. Finally, the same trends are observed for the BGAs investigated here over a variety of aging temperatures, shown in Table 7 and Figure 7.

Table 7. Characteristic Life for SAC 305 BGA Aging over 12 Months with Varying Package Sizes

Package Size \ Aging Temp.	NA	25℃	55℃	85℃	125℃
19	4718	3905	2871	2687	2215
15	3742	3096	2246	2107	1884
10	3328	2937	2155	1874	1551
5	5170	4265	3708	3455	3012

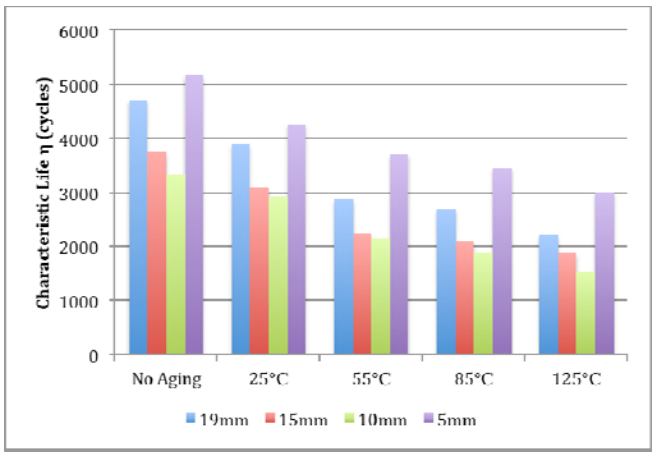

Figure 7. Degradation chart for SAC305 BGA reliability after aging over 12 months using varying package sizes and aging temperatures.

Figure 8 shows the degradation behavior for SAC 10mm BGAs aged at 125°C, while Figure 9 shows the characteristic life comparison for 10mm BGAs with different solder alloys and board finishes subjected to 125°C.

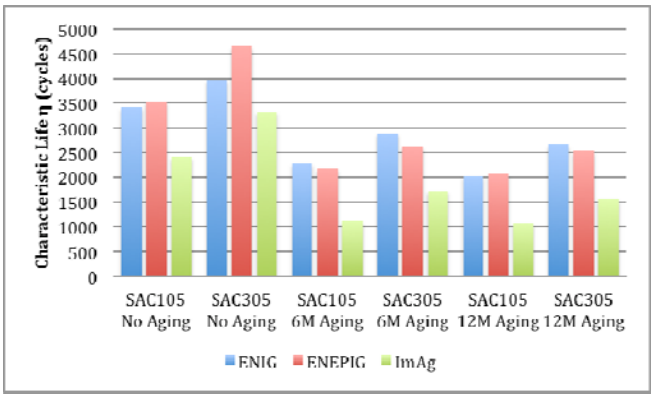

Figure 8. Degradation chart for SAC 10mm BGA reliability after aging at 125°C for various aging times.

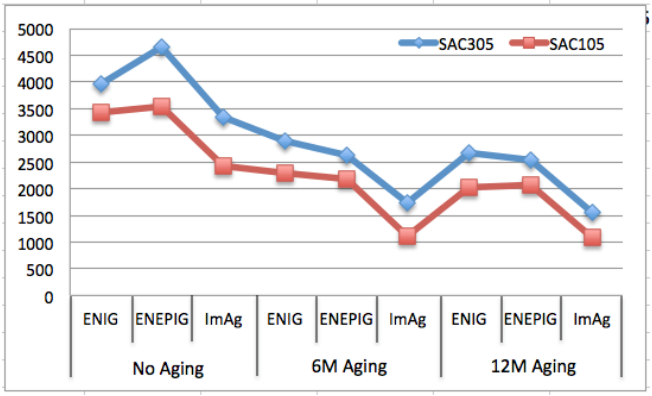

Figure 9. SAC105 and 305 characteristic life for the 10mm BGA vs. board finish and aging time (aging at 125°C)

Figure 8 shows that BGA packages with ENIG and ENEPIG surface platings perform better both before and after isothermal aging than BGA packages with ImAg surface finish. Figure 9 adds that SAC 105 solder joints perform worse than SAC305 in all cases, illustrating the risk when using SAC105 in applications where thermal fatigue failure is a concern.

Failure Analysis

Cracks in solder joints cause increasing electrical resistance and eventual open circuits in BGA components. During thermal aging and cycling, the solder joint undergoes deformation due to the thermal expansion (CTE) mismatch between the solder joint and the printed circuit board (PCB) and the component, as well as local CTE differences between grains within the solder. Solder microstructural changes include intermetallic compound (IMC) layer growth at PCB/solder joint/package interface or along grain boundaries in the solder bulk and grain coarsening over time and temperature. The IMC layer is relatively brittle and, over time/temperature, consumes a larger fraction of the solder ball, so cracks are favored to propagate along them and finally cause solder joint failure. Solder recrystallization is also frequently observed in fatigue failures wherein cracks are formed away from the solder interfaces and along the recrystallized grains within the bulk of the solder at positions where the stress/plastic work is high.

A detailed failure analysis for aged SAC alloys in BGA packages as a function of the surface finishes used here has been given in a previous publication [11]. For the present work, we have focused on the IMC growth kinetics under the complex thermal history (aging + cycling) utilized in aging/fatigue tests.

Figure 10 shows the starting (non-aged) ENIG AND ENEPIG layer structure elucidated by Rutherford backscattering spectroscopy (RBS). The starting board finish interlayers are relatively sharp, each with a 750 Å Au layer and a 3 µm layer of Ni. For ENEPIG, the added Pd interlayer is 1450 Å in thickness.

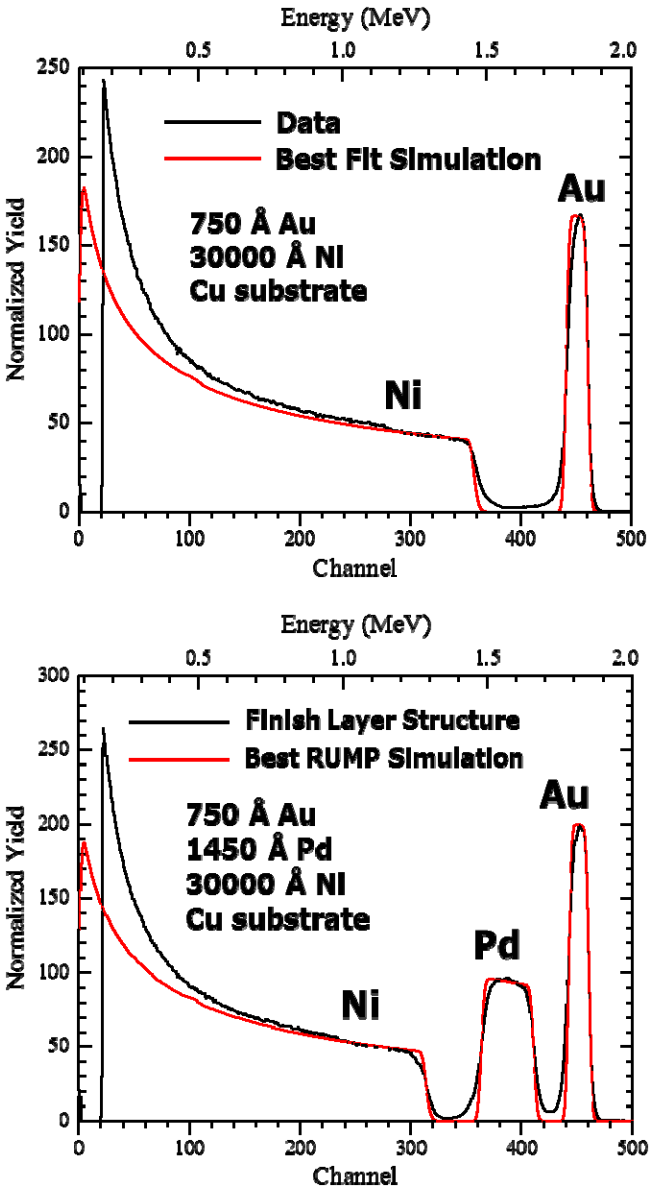

Figure 10. RBS spectrum illustrating the starting (before aging) layer structure of the ENIG and ENEPIG board finishes. The slight rounding of the spectra compared to the best simulation indicates a slight amount of inter-diffusion between the layers.

For SAC solder systems with ImAg plating, typical IMC layers are Cu_6Sn_5 and Cu_3Sn at the Sn/Cu interface and Ag_3Sn in the solder bulk [7]. Initially Cu_6Sn_5 forms adjacent to the copper layer during the reflow process, then during isothermal aging and cycling, Cu_3Sn forms by solid-state diffusion between the copper pad and the Cu_6Sn_5 layer. For SAC solders with ENIG/ENEPIG plating, the IMC layer becomes $(Cu,Ni)_6Sn_5$ and $(Cu,Ni)_3Sn$ [10]. The presence of the nickel layer in ENIG/ENEPIG acts as a diffusion barrier, which retards Cu dissolution into the solder to insure better reliability. Figure 11 shows the board-side IMC region for the case of SAC305 on ENEPIG.

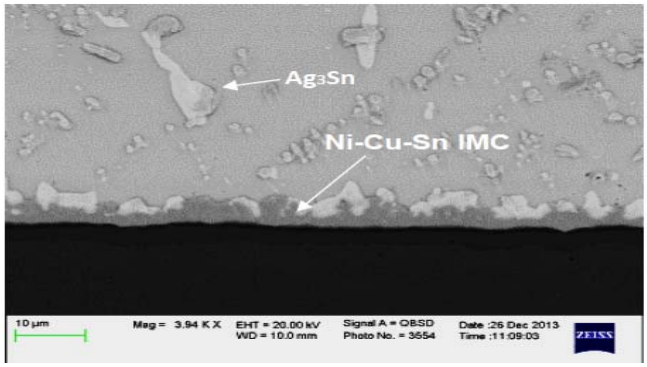

Figure 11. SEM micrograph of the IMC region of SAC305 solder joint on ENEPIG surface plating after 12 months/125°C aging.

Different solder joint failure modes observed in this study are shown in Figure 12. Cracks were observed to propagate near both board- and package-side intermetallic layers and through the bulk of the solder alloy in a few cases.

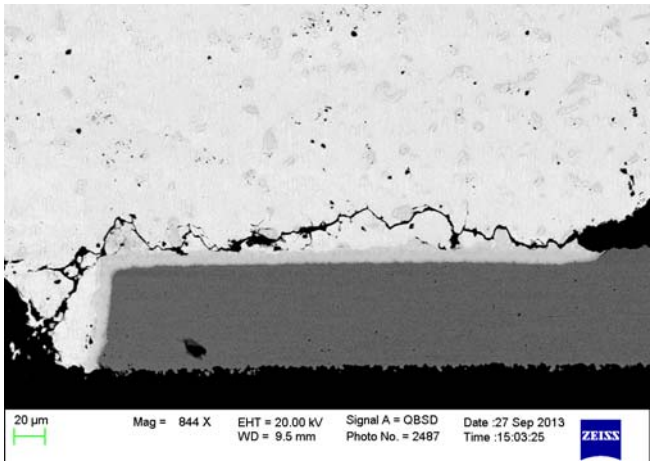

(a)

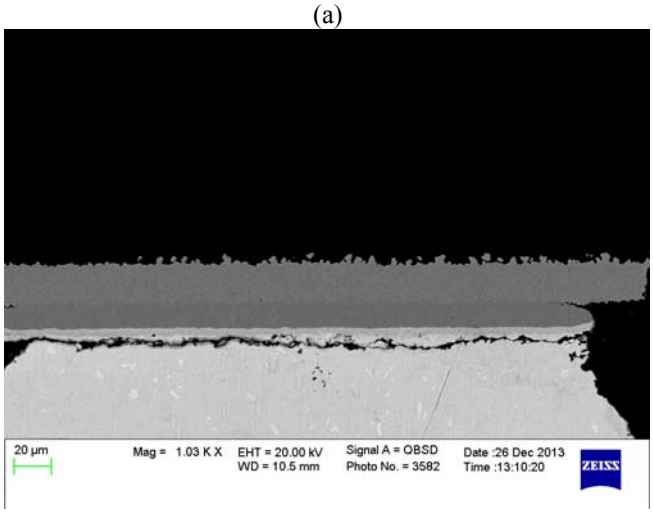

(b)

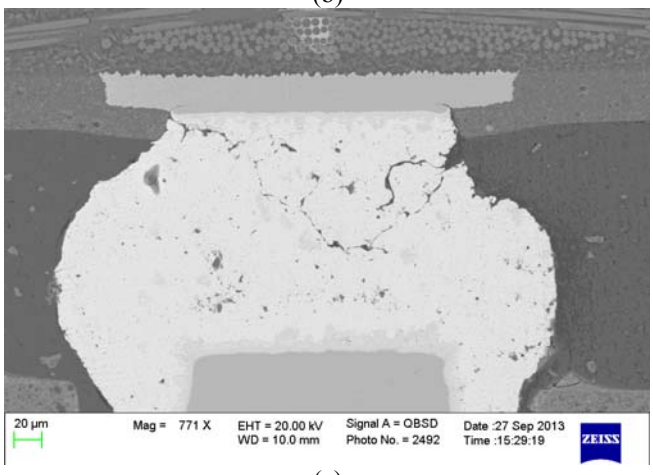

(c)

Figure 12. Representative solder joints failure modes. Crack propagation close to the (a) board-side IMC layer and the (b) package-side IMC layer. (c) Crack propagation through the solder bulk.

IMC Layer Thickness Analysis

Because solder joint failure is frequently associated with the extent of IMC formation, we routinely measure the thickness of the IMC region over time and temperature. Since the thickness is difficult to measure due to the scalloped nature of most IMC films, we average three measurements along the intermetallic layer for three solder balls, located at a left, center, and right corner line under a package. Table 8 shows the total IMC layer thickness for BGAs subjected to different aging times.

Table 8. IMC Layer Thickness for 0.8mm Pitch BGA over Aging (125°C) Time on ImAg.

Aging Time \ Solder Alloy	SAC105 (µm)	SAC305 (µm)
No Aging	1.7	1.8
6 Months	6.7	6.5
12 Months	8.0	9.0
24 Months	11.6	13.9

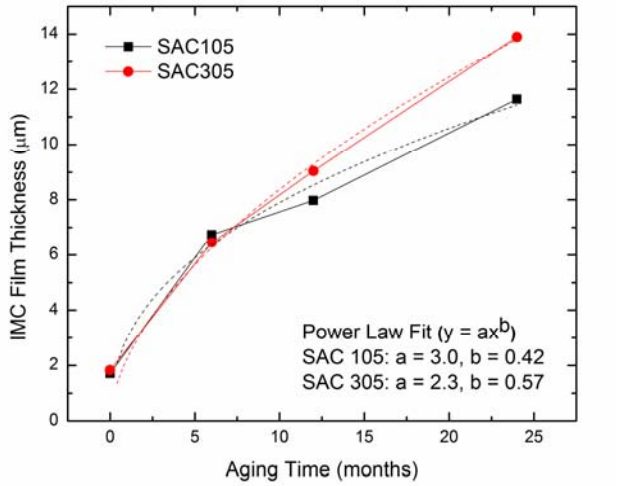

Figure 13. Total IMC film thickness vs. aging time for SAC 105 and 305 on ImAg surface plating.

The dotted curves show the best fit to a power law function $y = ax^b$. The values of b near 0.5 indicate parabolic or diffusion-controlled growth. The value of a is proportional to the diffusion constant of Cu through Sn.

Figure 13 shows that the IMC layer thickness for both SAC105 and SAC305 increases significantly during thermal aging and cycling, but that the rate of increase slows markedly after the first six months of aging. This behavior is reminiscent of diffusion-controlled growth, which predicts a $\sim t^{0.5}$ dependence of film thickness vs. time t (at constant temperature). The fact that the IMC growth is fairly close to $t^{0.5}$ behavior for such a complex thermal environment (isothermal aging + thermal cycling) indicates that the IMC growth depends more on the (isothermal) aging treatment and less on the thermal cycling treatment.

CONCLUSION

Long-term isothermal aging in elevated temperature has a severe impact on the reliability of SAC solder joints. Two-parameter Weibull plot shows that the reliability of BGA

packages degrades up to 70% after two years of aging at elevated temperature (125°C). With increases in aging time and temperature, the reliability of BGA components degrades more. For BGAs with identical ball alignments, packages with large solder balls have better reliability. Further, BGA packages with full array ball alignments performs better than perimeter ball alignments. BGA packages with ENIG and ENEPIG surface plating yields better reliability after isothermal aging than BGA packages with ImAg surface finish. Microstructural evolution and deformation during thermal aging and cycling causes solder joint failure. For the SAC/ImAg system, the typical IMC layers are Cu_6Sn_5 and Cu_3Sn at the Sn/Cu interface and Ag_3Sn inside the solder bulk. For the SAC/ENIG/ENEPIG system, the IMC layer becomes $(Cu,Ni)_6Sn_5$ and $(Cu,Ni)_3Sn$. The thickness of the IMC layer grows roughly as a $\sim t^{0.5}$ dependence during isothermal aging and thermal cycling.

ACKNOWLEDGEMENTS
This work was supported by the Center for Advanced Vehicle Electronics and Extreme Environment Electronics (CAVE3).

REFERENCES

[1] M. A. Matin, W. P. Vellinga, M. G. D. Geers. "Thermomechanical Fatigue Damage Evolution in SAC Solder Joints," Mat. Sci. and Eng. A 445–446, pp. 73–85, 2007.

[2] M. Berthou, P. Retailleau, H. Frémont, A. Guédon-Gracia, and C. Jéphos-Davennel, "Microstructure evolution observation for SAC solder joint: Comparison between thermal cycling and thermal storage," Microelectron. Rel., vol. 49, nos. 9–11, pp. 1267–1272, Sep./Nov. 2009

[3] M.A. Matin, E.W.C. Coenen, W.P. Vellinga, M.G.D. Geers, "Correlation between thermal fatigue and thermal anisotropy in a Pb-free solder alloy," Scripta Materialia 53 (2005) 927–932.

[4] Tae-Kyu Lee, Hongtao Ma, Kuo-Chuan Liu, and Jie Xue, "Impact of Isothermal Aging on Long-Term Reliability of Fine-Pitch Ball Grid Array Packages with Sn-Ag-Cu Solder Interconnects: Surface Finish Effects," J. Elect. Mat., Vol.39, No.12, 2010.

[5] J. Zhang, Z. Hai, S. Thirugnanasambandam, J. L. Evans, M. J. Bozack, Y. Zhang, J. C. Suhling, "Aging Effects on Creep Behaviors of Lead-Free Solder Joints and Reliability of Fine-Pitch Packages," Proc. Surface Mount Technology International Conference, 2012.

[6] J. Zhang, Z. Hai, S. Thirugnanasambandam, J.L. Evans, M. J. Bozack, "Correlation of Aging Effects on Creep Rate and Reliability in Lead Free Solder Joints," Journal of Surface Mount Technology, (2012). Vol. 25 (3), pp. 19-28 Orlando, FL.

[7] J. Zhang, Z. Hai, S. Thirugnanasambandam, J. L. Evans, M. J. Bozack, Y. Zhang, J. C. Suhling, "Thermal Aging Effects on the Thermal Cycling Reliability of Lead-Free Fine Pitch Packages," IEEE Trans. Compon. Packag. Manuf. Technol., vol. 3, pp. 1348 – 1357, 2013.

[8] Z. Hai, J. Zhang, Chaobo Shen, J. L. Evans, and M. J. Bozack, " Long Term Aging Effects on Reliability Performance of Lead-Free Solder Joints," Proc. Surface Mount Technology International Conference, 2013.

[9] Chaobo Shen, Z. Hai, Cong Zhao, J. Zhang, J. L. Evans, and M. J. Bozack, "The Effect of Isothermal Aging on the Reliability of Sn-Ag-Cu Solder Joints Using Various Surface Finishes," Proc. Surface Mount Technology International Conference, 2014.

[10] J. W. Yoon, B. I. Noh, J. H. Yoon, H. B. Kang, S. B. Jung, "Sequential Interfacial Intermetallic Compound Formation of Cu_6Sn_5 and Ni_3Sn_4 between Sn-Ag-Cu Solder and ENEPIG Substrate During a Reflow Process," J. Alloys and Compounds 509, pp. L153-L156, 2011.

[11] Z. Hai, J. Zhang, C. Shen, J. L. Evans, M. J. Bozack, M. M. Basit, and J. C. Suhling, "Reliability Comparison of Aged SAC Fine-Pitch Ball Grid Array Packages vs. Surface Finishes," IEEE Trans. Compon., Packag., Manuf. Technol., vol. 5, no. 6, pp. 828-837, June 2015.